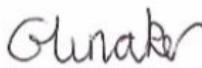# UNIVERSITY OF EXETER

I2 Report

Implementation and Analysis of Turbulent Atmospheric Boundary Layer Flow for an Actuator Disk Wind Turbine Model

George Hyde-Linaker

2015
4th year MEng Group Project

I certify that all material in this thesis that is not my own work has been identified and that no material has been included for which a degree has previously been conferred on me.

Signed.............................. Glinaker ....

College of Engineering, Mathematics, and Physical Sciences
University of Exeter

I2 Report

ECMM102

Title: Implementation and Analysis of Turbulent Atmospheric Boundary Layer Flow for an Actuator Disk Wind Turbine Model

Word count: 11079
Number of pages: 40

Date of submission: Thursday, 28 April 2016

Student Name: George Hyde-Linaker
Programme: MEng Mechanical Engineering
Student number: 620010141
Candidate number: 026912

Supervisor: Gavin Tabor

Abstract

One significant issue currently in the wind energy sector is the difference between the modelled and observed power generated by offshore wind farms. This power discrepancy exists due to the complex aerodynamic interactions in wind farms being difficult to model. The modelling of these interactions is predominantly undertaken using computational fluid dynamics (CFD). The characteristics of the airflow subjected to wind turbine models in CFD are a possible contributor to the power discrepancy, as approximations to the complex airflow are used to reduce the computational cost of simulations. This project presents a method of generating an accurate and representative simulation of the neutral atmospheric boundary layer (ABL) for the purpose of accurately modelling of the behaviour wind turbines within OpenFOAM.

The profile of the ABL modelled in OpenFOAM was obtained through the wind tunnel experimentation of an induced boundary layer that aimed to replicate the boundary layer generated at offshore wind farm locations. Synthetic turbulence was then imposed onto this mean profile via the Synthetic Eddy Method (SEM) to create an approximation to a turbulent ABL. The SEM was then modified to incorporate the behaviour of an actuator disk wind turbine model (ADM) for assessing if the performance of the ADM is significantly influenced by the airflow of the turbulent ABL. This investigation used Large Eddy Simulation (LES).

The main outcome from the project was the production of the previously mentioned SEM in OpenFOAM, which was used to produce an ABL that correlated well with the boundary layer generated in the wind tunnel experimentation. This SEM was also successfully modified to incorporate an ADM. However, the conclusions drawn from using this modified SEM for investigating its effect of ADM performance were somewhat limited. The model provided significant results when analysing the wakes of the ADMs, but no strong conclusions could be drawn from assessing the power predicted to be generated by the ADMs.

Keywords:

Atmospheric boundary layer, Wind energy, OpenFOAM, Large Eddy Simulation, Wind turbine, Synthetic Eddy Method

Table of contents

1. Introduction and background

1.1.   Introduction and Background

Horizontal axis wind turbines (HAWTs) utilised in large offshore arrays known as wind farms, are a major contributor to global energy generation. The energy harnessed from wind farms is currently the most cost-effective alternative energy source and is nearly competitive with the traditional sources. Therefore it is necessary to accurately predict the energy generated from wind turbines, these predictions are predominantly achieved via computational fluid dynamics (CFD). However current CFD modelling techniques for wind turbine modelling struggle to accurately predict the energy generated by wind turbines, this is due to the complex aerodynamic interactions associated with the airflow subjected to and produced by wind turbines. One particular aspect of the aforementioned complex aerodynamics is the atmospheric boundary layer (ABL). This project aims to investigate the most suitable method for modelling the turbulent airflow of the ABL and to assess its effect on the actuator disk wind turbine model (ADM).

Simulating the behaviour of the ADM is often completed using Reynolds-averaged Navier-Stokes (RANS) turbulence modelling, however this approach can be insufficient as RANS modelling can only yield a time averaged mean value for the velocity field without the turbulent fluctuations that exist in the flow. This is particularly evident in the wakes generated by RANS modelling of ADMs. In order to obtain a better approximation to the transient flow within the simulations, the modelling in this project used Large Eddy simulations (LES).

LES modelling is also necessary for modelling the profile and turbulence of ABL flow. For the scope of this project, synthetic turbulence was imposed onto a mean ABL velocity profile for approximating the turbulent ABL. The Synthetic Eddy Method (SEM) was the method used for this. The SEM creates eddies of a prescribed characteristic length scale in a specified region of the computational domain, imposing these eddies onto a mean ABL flow gives a physical approximation to turbulent ABL flow. The turbulence generated by using the SEM emulates the model of turbulence as a superposition of coherent structures, this gives SEM a qualitative benefit over other comparable methods which either do not incorporate eddies or which simplifies their effect and behaviour.

1

For to the scope of this project it was also necessary to simultaneously model the turbulence within the ABL and the behaviour of an ADM. In order to achieve this a modified version of a SEM was developed over the course of the project to incorporate an ADM. This modified SEM solver has the capability of modifying the geometry and characteristics of the actuator disk, as well as the sub-domain in which eddies are generated in and their characteristics. This solver was named *EddiesAndActuatorDiskPisoFoam (EAADPF)* and was used for fulfilling the aims and objectives of this project.

1.2.   Group Project

The main aim of the group project associated with this work was to evaluate existing wind farm modelling techniques and to develop improved modelling techniques that will reduce the discrepancy between the modelled and observed power generated by wind farms. The work conducted in this paper contributes to this overall group aim by suggesting the most suitable method for generating the turbulent ABL for wind turbine modelling, and by assessing turbine performance when using the modelled turbulent ABL as opposed to a uniform inlet velocity. This information can then be used for future reference.

1.3.   Aims and Objectives

In addition to implementing *EAADPF* within OpenFOAM, the model should also run at a reasonable computational cost. This is so that the solver will have a wider range of use than other high fidelity ABL solvers that require sophisticated computational resources. This project also presents the experimentation of an induced boundary layer in a wind tunnel that mimics the profile of an offshore neutral ABL. This experimental data was then used as a reference for generating the ABL profile for the CFD simulations in this work.

The aims for this paper can be summarised in the project objectives, defined as:

- Approximate the velocity profile of an offshore ABL via wind tunnel experimentation
- To incorporate an ADM into the domain of the turbulent ABL by modifying a SEM
- To assess the impact of using turbulent ABL flow on turbine performance as opposed to a constant uniform inlet velocity

2. Literature review

For the purposes of this paper there are several areas of prior literature that are highly relevant. This literature ranges from the ADM produced by Svenning (2010) [1] to the SEM proposed by Jarrin et al. (2006) [2].

2.1.   OpenFOAM

The CFD simulations in this project were completed in OpenFOAM (Open Field Operation And Manipulation), a C++ toolkit of classes that run in Linux. These classes are used for writing continuum mechanics computationally and can be used for solving fluid flow cases. OpenFOAM contains a library of pre-made solver applications that can solve the majority of fluid flow cases. Additionally, OpenFOAM is an open-source code and is suitable for implementing the SEM despite it not being a generally accessible application. Furthermore, studies such as Lignarolo et al. (2011)[3] and Sumner (2010)[4] have used OpenFOAM for simulating the ABL; this validates OpenFOAM as a suitable package for the ABL simulations within this project. Due to no prior use, a vast number of OpenFOAM tutorials were studied and practiced at the commencement of the project.

2.2.   The Atmospheric Boundary Layer (ABL)

2.2.1. The ABL in General

In modern engineering it is well known that a boundary layer is created when a moving fluid meets a solid boundary, and hence a boundary layer is created as atmospheric air moves over the Earth's surface. The resulting boundary layer from this interaction is known as the atmospheric boundary layer (ABL). As the ABL is in the lowest kilometres of the earth's atmosphere it is a vital factor when predicting the aerodynamics associated with wind turbines computationally.

The ABL is described as the region of the atmosphere where the airflow is directly affected by the thermal and physical effects of the earth's surface. Garratt (1992)[5] presents an extensive overview of the varying aspects of the ABL, defining it as the region of the atmosphere where airflow is significantly affected by the local topography, upstream airflow and the exchange of momentum and heat at the earth's surface. In addition to this, it is also noted the importance of

stratification when considering the structure of the ABL with respect to wind turbine modelling.

As discussed in Holdaway et al. 2011[6], the structure of an ABL varies diurnally because of the effects of stratification. ABLs are generally classified as either stably stratified, convective or neutrally stratified. A neutral ABL profile presumes the temperature to be constant throughout the boundary layer, whereas the other ABLs are influenced by temperature fluxes. Modelling the effects of varying temperature fluxes within ABL airflow is very computationally expensive and beyond the scope of this project, in which a neutral boundary layer will be considered. Blessmann (1973)[7] presents a detailed description of the neutral atmospheric boundary layer its associated wind characteristics.

2.2.2. ABL Modelling and ABL Turbulence

The majority of prior studies which involve modelling the ABL and its associated turbulence such as Churchfield et al. (2010)[8], Andren et al. (1995)[9] and Stoll (2006)[10] all have used LES for resolving the fluid flow. This is mainly due to the ranging spatial and temporal scales of eddies within ABL flow. The range of scales means that explicit solving of atmospheric airflow by Direct Numerical Simulation (DNS) is far too computationally expensive, especially for the scope of this project. Reynolds-averaged Navier-Stokes (RANS) simulations would be more practical for resolving ABL flow, but resolve fluid motion by time averaging and by using a turbulence model to reduce the dynamic complexity of the flow. The resolved flow from a RANS simulation is therefore a mean averaged result without the presence of eddies, and therefore not representative of the actual turbulent flow within the ABL. Chang et al. (2004)[11] also indicates this approach is not suitable, stating that RANS turbulence models overestimate and miscalculate the degree of turbulence within eddies. As such, in this project, the fluid flow of the ABL and the ADM were modelled using LES.

Ferziger (1999)[12] presents an extensive overview of LES and its applications. LES is a technique by which the scales of the flow are spatially filtered. The larger (and more important) scales of the flow are explicitly solved and the scales of flow at the sub-grid level are modelled using a sub-grid scale turbulence model, as they are heavy to compute. Using LES consequently simulates the ABL profile with the presence of eddies within the flow whilst reducing the prohibitive computational cost of DNS simulations. Figure 1 shows a schematic representation of the range of eddy scales that may exist in a fluid flow and the differing scales
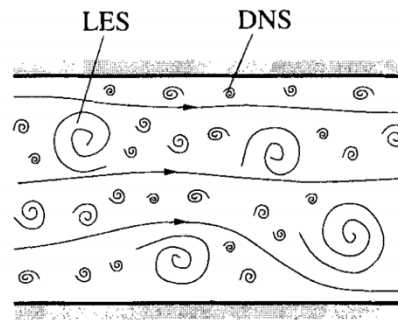
4

which LES and DNS may explicitly solve.

Figure 1. – Schematic representation of range of eddy scale in fluid flow [12]

2.3.   Synthetic Eddy Method

Utilising LES modelling for simulating spatially developing flows such as ABL flow necessitates the specifying of realistic inlet boundary conditions for obtaining an accurate numerical simulation. In RANS simulations, it is only necessary to consider mean time-averaged approximations of the airflow properties, making inlet conditions relatively easy to specify. However for LES, the inflow data generated is much more significant due to turbulent and unsteady inflow conditions needing to be prescribed. In this project the SEM was used for this by superimposing eddies of a prescribed length scale onto a mean ABL flow. The SEM was considered as the most suitable method for generating synthetic turbulence as it constructs eddies from a turbulent length scale, as opposed to other methods that are very dependent on experimental data and mathematical theory.

Jarrin et al. (2006)[2] presents a widely referenced version of the SEM, which provides an outline of the SEM used in this project. The main benefits of SEM which apply to this project are that the SEM is very adjustable and is easily scalable, meaning the meshed domain does not need to be especially fine to produce a reasonably accurate solution. This is useful for the limited scope and timeframe of the project. The concept of the SEM proposed in Jarrin et al. 2006[2], and elaborated on in Jarrin et al. (2008)[13] was implemented in Richmond (2015)[14] for simulating atmospheric airflow over the Humber bridge by creating the solver *eddyPisoFoam*. This solver was modified and implemented in this project and then used for approximating turbulent ABL flow; it was then further modified to incorporate the modelling of the ADM. This modified SEM has a reasonable computational cost and is easily implemented, additionally the generated data displayed good length and time scales.

2.4.   NREL ABLSolver

As part of the National Renewable Energy Laboratory (NREL), Churchfield et al. 2014[15] documents a series of solvers for various aspects of wind turbine modelling in OpenFOAM. Amongst these are two solvers documented as 'ABLSolver' and 'ABLTerrainSolver'. For the purposes of this project the ABLSolver was studied. The role of ABLSolver is to initialise a wind farm domain with the precursor ABL volume field; this data is then subjected to an array of actuator line models (ALMs) to obtain the aerodynamics of the wind farm array. Unfortunately, due to the complexity of the solver, the computational resources available and the time restrictions of the project, the simulated ABL domain obtained from an ABLSolver simulation was not used for the modelling of the wind farm array and was only used for the comparing the data of the ABL profiles in this project. The ABLSolver is a very high-fidelity solver, modelling factors such as buoyancy, temperature and the Coriolis force due to planetary rotation. This will be elaborated on in the theory section.

2.5.   Wind Tunnel ABL Experimentation

Simulating an ABL profile via wind tunnel experimentation is severely limited by the working test section dimensions of the wind tunnel being used. This is mainly due to the difficultly in simulating the thickness of the ABL in small-scale wind tunnels such as in the University of Exeter aerodynamics lab. The use of passive devices such as roughness elements and spires can help to overcome this issue. The general experimental setup of these devices within the wind tunnel for exaggerating the boundary layer profile is shown in figure 2, in Irwin (1980)[16].
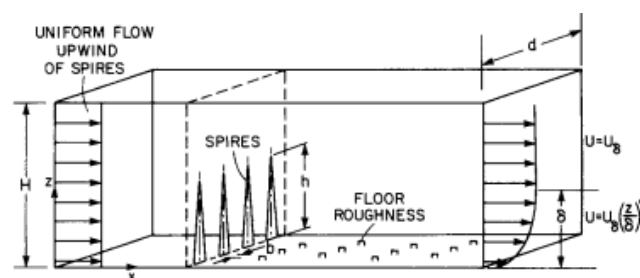
Figure 2. – Experimental setup of boundary layer generation in wind tunnel [16]

The concept of combining spire arrays with floor roughness elements for approximating the structure of an ABL originated in Campbell et al. (1969)[17] and Counihan (1979)[18] when the generated downstream velocity profiles were shown to have a likeness to the general form and turbulence present within an ABL. Both studies used spires approximately the height of the

6

boundary layer, roughness elements at the tunnel floor and a castellated barrier wall to generate an initial momentum deficit to the boundary layer. These features can all be modified to generate the desired boundary layer profile.

Turbulent eddies are formed as air flows over the roughness elements, resulting in turbulence and a velocity gradient, much like actual terrains. To overcome the issue of limited fetch lengths for the roughness elements in small-scale wind tunnels, Counihan (1979)[18] used spires as vortex generators. Spires thicken the generated boundary layer and help to create a velocity profile with the desired Hellman exponent value; they also make the boundary layer more measurable. The study on which the experimentation in this project was based was Hobson-Dupont (2015)[19], which presents recent study into the previously described techniques.

2.6.   *Actuator Disk Wind Turbine Model*

Due to practically and computational expense, resolving the flow around turbine blades is usually not feasible and actuator methods are used for approximating fluid-turbine interactions, in this project the ADM was used. The ADM is a commonly used wind turbine model in industry and has been used in wind turbine studies such as Mikkelsen (2003)[20] and Sanderse (2009)[21]. Horlock (1978)[22] outlines the theory and origins of the actuator disk concept, which dates back to the work of Rankine and Froude.

Actuator disks are artificial devices that are used to transform the flow at a specified region within the computational domain, and hence can be set to mimic the energy extraction process of wind turbines. This approach provides a reasonable model of the turbine's behaviour; the momentum transported between the turbine and the fluid is predicted and added to the fluid within the actuator disk as a volume source. This information can then be used to predict the energy generated by a wind turbine.

In this project the ADM purposed in Svenning (2010)[1] was used for approximating the behaviour of wind turbines. Svenning (2010)[1] presents an implementation of an actuator disk, this actuator disk and its effect on the airflow can be seen in figure 3. The Svenning model works by computing the volume force from the performance code of the disk, where the disk performance is dependent on the flow variables in the region close to the actuator disk. The volume force of the disk varies with respect to the radial direction and is calculated via a prescribed thrust and torque is imposed on the fluid. Additionally, the model incorporates thrust

7

and swirl into the actuator disk region, helping to produce a wake region downstream of the disk.
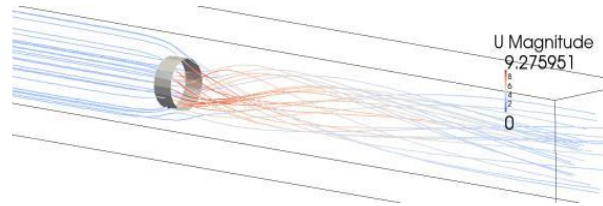

Figure 3. – Actuator disk implemented in Svenning[1]

2.7. *Control Volume*

In order to compute the power predicted to be generated by the ADM, a cuboidal control volume can be used to calculate the change in flux across the region of the actuator disk. This is possible due to the Conservation of Liner Momentum; the momentum flux on each face of the control volume can be calculated and computed to yield the power generated by the turbine model by evaluating the energy lost from the flow. This approach to gauging the energy produced by a turbine model was used in this project, a prior use of this approach is presented in Gebreslassie (2012) [23].

3. Theoretical background and Methodology

3.1. *Governing Equations and RANS modelling*

As is widely known the main equations that govern and apply to all fluid flows are the Navier-Stokes equations. For the scope of this project, incompressible flow is being considered. The Navier-Stokes equations for incompressible flow comprise of the continuity equation, equation 1, and the momentum equations shown in equation 2.

$$\frac{\partial u_i}{\partial x_i} = 0 \qquad \text{- Equation 1.}$$

$$\frac{\partial u_i}{\partial t} + \frac{\partial (u_i u_j)}{\partial x_j} = -\frac{1}{\rho}\frac{\partial p}{\partial x_i} + \frac{\partial}{\partial x_j}\left[v\left(\frac{\partial u_i}{\partial x_j} + \frac{\partial u_j}{\partial x_i}\right)\right] + f_i \qquad \text{- Equation 2.}$$

Where ρ, v and p are the density, kinematic viscosity and pressure of the fluid respectively. x_i and x_j denote the components of the coordinate system, u_i and u_j signify the velocity components and f_i represents the body forces on the fluid.

8

In order to resolve the fluid motion within the computational domain, the Navier-Stokes equations are numerically simulated by the finite volume method via CFD. For this project the CFD simulations resolved the flow using LES and RANS modelling. LES modelling was the most used approach for modelling the interaction between the turbulent ABL and the ADM, although it was found that an initial RANS simulation using the k-epsilon model reduced the simulation run time.

3.2.   Large Eddy Simulation (LES)

As mentioned, LES spatially filters the fluid flow and involves the explicit calculation of large scale eddies and the modelling of eddies at the sub-grid scale. Therefore the equations that govern LES are a combination of filtered Navier-Stokes equations and source terms. The governing equations for LES and their formulation are covered in depth in Sagaut et al. 2005[24] and will only be outlined in this paper. The filtering of the Navier-Stokes equations in LES modelling is necessary for differentiating the velocity fields that contain large scale eddies to that of sub-grid scale eddies. The filtering of the Navier-Stokes equations yields the equations described in equations 3 and 4. As the continuity equation is linear, filtering does not affect it.

$$\frac{\partial \bar{u}_i}{\partial x_i} = 0 \qquad \text{- Equation 3.}$$

$$\frac{\partial \bar{u}_i}{\partial t} + \frac{\partial}{\partial x_j}\left(\overline{u_i u_j}\right) = \frac{-1}{\rho}\left(\frac{\partial \bar{p}}{\partial x_i}\right) + v\frac{\partial}{\partial x_j}\left(\frac{\partial \bar{u}_i}{\partial x_j} + \frac{\partial \bar{u}_j}{\partial x_i}\right) \qquad \text{- Equation 4.}$$

Where $\bar{u}$ and $\bar{p}$ are the filtered velocity and pressure respectively, p is the pressure and v is the kinematic viscosity. And x_i and x_j denote the components of the coordinate system, u_i and u_j.

Furthermore, the filtered velocity field in LES can be defined one-dimensionally as in equation 5, where $G(x, x')$ is a localised function known as the filter kernel. This filtration operation was proposed in Leonard (1974)[25].

$$\bar{u}_i(x) = \int G(x, x') u_i(x') dx' \qquad \text{- Equation 5.}$$

For the LES modelling in this project the Smagorinsky turbulence model was used for resolving the fluid flow at the sub-grid scale.

3.3.   ABL Profile and Wind Tunnel Experimentation

ABL profiles are often compared using the wind profile power law. The wind profile power law, shown in equation 6, is the relationship between the relative mean horizontal wind speed at a certain height against that of another.

$$\frac{u}{u_r} = (\frac{z}{z_r})^\propto$$ - Equation 6.

Where u is the horizontal wind velocity at height z, u_r is the horizontal wind velocity at the height z_r and $\propto$ is the Hellman exponent.

Typical values of the Hellman exponent for differing locations and differing ABL structures are shown in table 1.

Table 1. – Table of Hellman Exponent values for differing ABLs and locations [26]

Location and ABL characteristics	$\propto$
Unstable air above open water surface	~0.06
Neutral air above open water surface	~0.10
Unstable air above flat open coast	~0.11
Neutral air above flat open coast	~0.16
Stable air above open water surface	~0.27
Unstable air above human inhabited areas	~0.27
Neutral air above human inhabited areas	~0.34
Stable air above flat open coast	~0.40
Stable air above human inhabited areas	~0.6

The value of the Hellman exponent value is often used in comparing the profiles of ABLs. As stated previously, the ABL profile generated in OpenFOAM was based on the induced boundary layer generated in the wind tunnel experimentation aspect of the project. With offshore wind turbine modelling being considered, the roughness elements used in the wind tunnel experimentation were kept as small as possible whilst producing a measurable boundary layer. The Reynolds number, Re is defined as $Re = u.l/\nu$, where u is velocity, l is the characteristic length scale and ν is the kinematic viscosity. The characteristic length scale in the experimentation was considered as the height of the roughness elements (1.5cm). This meant that the Reynolds number of the flow was limited, and a wind velocity of $5.5ms^{-1}$ was used to ensure that the Reynolds number was not reduced so much that the surface was no longer aerodynamically rough. The kinematic viscosity of the air was presumed to be $1.3 \times$

10^{-5}, making $Re = 6346$. The constructed spires and roughness elements used for the wind tunnel experimentation in this project and its designed dimensions are shown in figure 4.
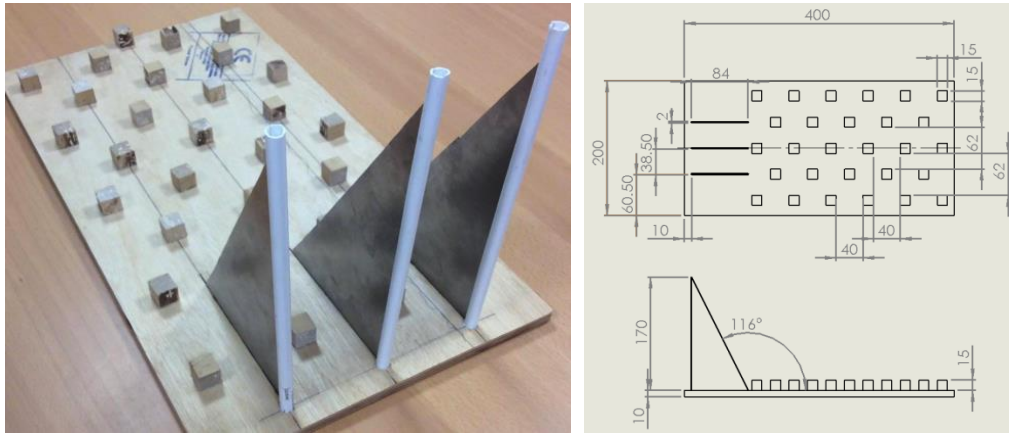

Figure 4. – Constructed board of roughness elements and design drawings

It was found that the most measureable boundary layer profile was at 40cm downstream of the trailing edge of the spires. In order to measure the velocity of the boundary layer at varying heights at this location, hotwire anemometry and a Pitot-static tube were used.

Hotwire anemometry produces an almost instantaneous reading of the temperature and the velocity of the airflow. It works due to the relationship between the velocity of the fluid being measured and the rate of convection from a stationary object in the flow to the fluid. The probe temperature is a few degrees above ambient, so as the fluid flows past the probe, heat is lost by convection. Therefore the faster the flow is, the rate of convection is higher.

Pitot-static tubes measure the pressure at a given location within the flow and are connected to a manometer. The velocity of the airflow can be found using the pitot-static tube measurements and the well-known manipulation of the Bernoulli Equation shown in equation 7, due to no differential in height being considered.

$$V_{measured} = \sqrt{\frac{2(p_{stagnation} - p_{static})}{\rho_{fluid}}}$$
- Equation 7.

In the wind tunnel experimentation the hotwire anemometer and the pitot static tube were found to correlate well, with a maximum differential of 7.1% between the readings. The pitot-static tube was therefore used for measuring the velocity of the airflow due to it being easier to log the wind speed data, the hotwire anemometer was used to ensure the reading were accurate.

In addition to calculating an ABL profile at offshore locations, the wind tunnel experimentation was also used as an opportunity for obtaining an approximation to the turbulence intensity within the ABL flow. This was done in order to compare the turbulence generated in CFD with that of the wind tunnel. The turbulence intensity of the ABL in the wind tunnel was calculated using the standard deviation of the velocity, shown in equation 8.

$$\sigma_A{}^2 = \frac{1}{N} \sum_{i=0}^{N-1} (u_i - \overline{u_i})^2 \qquad \text{- Equation 8.}$$

Where σ_A is the standard deviation, u_i is the measured horizontal velocity and $\overline{u_i}$ is the mean velocity. Using the standard deviation, equation 9 was used to calculate the turbulence intensity, I, of the airflow.

$$I = \frac{\sigma_A}{\overline{u_i}} \qquad \text{- Equation 9.}$$

From literature, turbulence intensity at typical wind turbine heights (~100m) typically varies by less than 10%, with the turbulence intensity typically varying between the values of 10-20% for a neutral ABL.

3.4. Synthetic Eddy Method

3.4.1. Procedure

The SEM is based on viewing turbulence as a superposition of eddies. By using the SEM, synthetic turbulence was introduced into the computational domain by generating a specified number eddies of a prescribed turbulent length scale in specific sub-region over the inlet plane of the domain. These eddies are defined by a shape function that encompasses the structure's spatial and temporal characteristics. The imposition of these eddies manipulates the velocity field within the sub-region in the domain and downstream of the eddy generation sub-region.

The procedure for generating turbulent fluctuations using the SEM can be described as follows:

1. Define the mean velocity, Reynolds stress tensor and the length scales of the flow.
2. Define sub-domain in which eddies are to be generated, which can be visualised in figure 5. Where the sub-domain is defined as:

$$[-\sigma_{x1}, \sigma_{x1}; -\sigma_{x2}, \sigma_{x2}; -\sigma_{x3}, \sigma_{x3}]$$
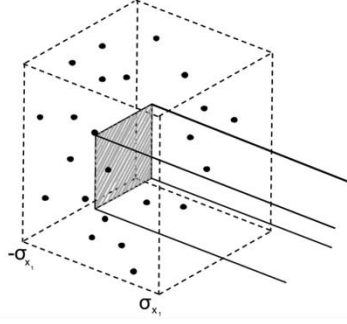
Figure 5. – Visualisation of Sub-domain (dotted), LES domain (solid), inlet (grey) and eddies (points)

3. Generate random position x^k and intensity ε_i^k for the eddies within the sub-domain.

4. Eddies are transported through the sub-domain with a reference velocity. The new position of a specific eddy is given by equation 10:

$$x_i(t + dt) = x_i(t) + U_0 dt \qquad \text{- Equation 10.}$$

When eddies leave the sub-domain, a new eddy of random intensity is generated at the opposite side of the sub-domain

5. Finally, turbulent fluctuations are computed as in equation 11:

$$u'_i(x) = \frac{1}{\sqrt{N}} \sum_{k=1}^{N} a_{ij} \varepsilon_j^k f_{\sigma(x)}(x - x^k) \qquad \text{- Equation 11.}$$

Where a_{ij} is the Cholesky decomposition of the Reynolds stress tensor as defined in equation 12, N is number of eddies, x is the position in the mesh, x^k is the position of eddy and the intensities ε_i^k are randomly generated as $\varepsilon_i^k \in \{-1, 1\}$, and $f_{\sigma(x)}$ is the shape function defined in equation 13.

$$a_{ij} = \begin{pmatrix} \sqrt{R_{11}} & 0 & 0 \\ R_{21}/a_{11} & \sqrt{R_{22} - a_{21}^2} & 0 \\ R_{31}/a_{11} & (R_{32} - a_{21}a_{31})/a_{22} & \sqrt{R_{33} - a_{31}^2 - a_{32}^2} \end{pmatrix} \qquad \text{- Equation 12.}$$

$$f_{\sigma(x)}(x - x^k) = \sqrt{V_B} \sigma^3 f\left(\frac{x_1 - x_1^k}{\sigma}\right) f\left(\frac{x_2 - x_2^k}{\sigma}\right) f\left(\frac{x_3 - x_3^k}{\sigma}\right) \qquad \text{- Equation 13.}$$

Where V_B is the volume of the sub-domain and $f(x)$ is the hat function, as in equation 14:

$$f(x) = \begin{cases} \sqrt{\dfrac{3}{2}}(1 - |x|), & \text{if } x < 1, \text{else} \\ 0 & 0 \end{cases} \qquad \text{- Equation 14.}$$

3.5.2. Guidelines for use

The turbulent length scale signifies the distance at which a cell can be affected by a given eddy, if cells are being influenced by many eddies the flow field is turbulent and therefore the selected turbulent length scale considerably affects the nature of the synthetic turbulence generated. The length scale should therefore be larger than or equal to the grid size or the generated eddies will be ineffective. Equation 15 shows a formula for a sensible length scale, σ. The length scale decided upon for this project was based on the average flow characteristics, using equation 15 as a guideline.

$$\sigma = \max(\min\left(\frac{k^{3/2}}{\varepsilon}, k\delta\right), \Delta) \qquad \text{- Equation 15.}$$

To ensure the continuity of the eddies passing through the domain, the shape of the sub-domain that eddies are generated is the same as the main computational domain, a box. So that the number of eddies within the sub-domain remains constant when eddies move out of range and are replaced by new random eddies on the opposite side of the sub-domain, this maintains a statistically even distribution of turbulence.

The necessary number of eddies in the domain depends on the selected eddy length scale as well as the size of domain. Equation 16 provides an approximation to the number of eddies required. This approximation take into account that the random positioning of the generated eddies in the sub-domain this can cause potential problems. For the SEM used in this project, the length scale and number of eddies are defined in *eddyProperties*.

$$N = \frac{V_B}{\sigma^3} \qquad \text{- Equation 16.}$$

3.5.   Methodology of Project

This section of the project outlines the methodology followed over the course of the project to fulfil the project aims in addition to the associated theory of elements of the project that have not been covered in this section thus far.

The three main objectives of the project were:

- Approximate the velocity profile of an offshore ABL via wind tunnel experimentation.

- To incorporate an actuator disk wind turbine model into the domain of the turbulent ABL by modifying an SEM solver.
- To assess the impact of using turbulent ABL flow as opposed to a constant uniform inlet velocity.

Implementation of the Actuator Disk Model

The first stage of the project was to implement the Svenning ADM in OpenFOAM 2.3.1. This implementation was achieved by modifying the C++ code for several of the case files and solver related files that were previously set up in OpenFOAM 1.5. The actuator disk is accounted for by the addition of a volume force in the region of the actuator disk. The properties of the actuator disk such as the geometry, torque and thrust are specified in *turbineProperties*. Due to this definition of the actuator disk, the implementation of a new ADM was achieved by using the solver modified to include the volume source, *actuatorDiskExplicitForceSimpleFoam.* This solver is a modified version of the *simpleFoam* solver, which has been adjusted to include an extra source in the U-equation. A velocity contour plot of the implemented ADM can be seen in figure 6. Figure 6 also shows the rotating flow in the wake of the actuator disk, this swirling of the flow downstream of the rotating actuator disk is partly due to the tangential force being present which adds swirl to the flow.
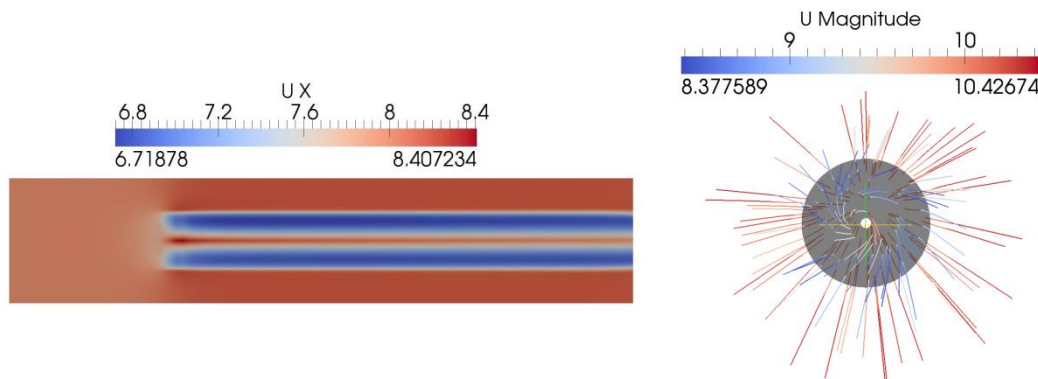
Figure 6. – Behaviour of Implemented Actuator Disk Model

For the purposes of using actuator disks for wind turbine modelling, the turbine is accounted for by adding momentum to the fluid flow explicitly. The momentum transported from the turbine to the fluid is predicted and added to the fluid within the actuator disk as a volume source. The volume force of the ADM in this project follows a Goldstein optimum distribution representing an ideal turbine operating at the Betz limit. To obtain this Goldstein optimum

15

distribution, the computing of the volume force in the axial and tangential direction uses similar expressions to those used in FINE^{TM}/Marine (2010)[27]. These equations are described in equations 17-20.

Where the constants A_x and A_θ are computed so that the volume force over the region of the actuator disk is equal to the prescribed torque, Q and thrust, T. The values of A_x and A_θ are computed as in equation 21 and 22.

$$f_{bx} = A_x r^* \sqrt{1 - r^*} \quad \text{- Equation 17.} \qquad f_{b\theta} = A_\theta \frac{r^*\sqrt{1-r^*}}{r^*(1-r'_h)+r'_h} \quad \text{- Equation 18.}$$

$$r' = \frac{r}{R_p} \quad \text{- Equation 19.} \qquad r^* = \frac{r'-r'_h}{1-r'_h} \quad \text{- Equation 20.}$$

$$A_x = \frac{105}{8} \frac{T}{\pi\Delta(3R_H + 4R_p)(R_p - R_H)} \quad \text{- Equation 21.}$$

$$A_\theta = \frac{105}{8} \frac{Q}{\pi\Delta R_p(R_p - R_H)(3R_p + 4R_H)} \quad \text{- Equation 22.}$$

As visible in figure 7, equations 17-20 calculate a volume force distribution which has a maxima between r = RH and r = RP, dropping to zero at r = RH and r = RP. This is a good approximation of the Goldstein optimum distribution of circulation.
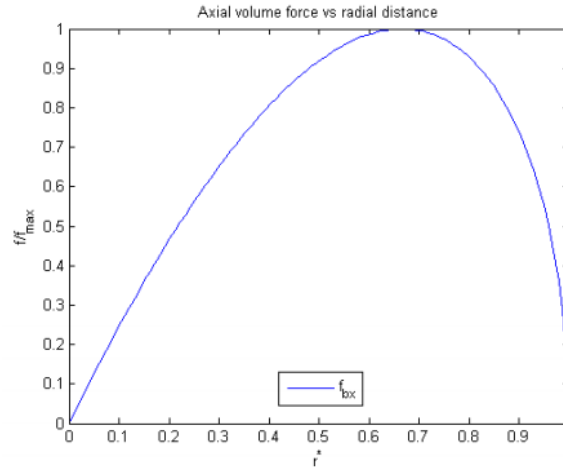

Figure 7. – Normalised volume force against Normalised radius [1]

Due to the scope of the project involving LES modelling for transient simulations, the solver *actuatorDiskExplicitForceSimpleFoam* was modified for PISO loop calculations, changing the solver into *actuatorDiskExplicitForcePisoFoam*.

ABL Profile generation in OpenFOAM

Accurate simulation of the entire height of the ABL profile requires accounting for the effects of temperature, humidity, buoyancy and the Coriolis force. Incorporating these factors into a solver, such as the ABLSolver developed by the NREL, results in the solver becoming very computationally expensive and not suitable for the timeframe of this project. Therefore for the scope of this project an ABL velocity profile 1000m high was only simulated for a limited height of 200m. From research it was assumed that the limited height of the ABL domain being considered would limit the effects of the Coriolis force being omitted. Investigating the accuracy of this approach will be considered as a source of further work.

To obtain and validate the ABL profile for this domain height, wind tunnel experimentation of an induced boundary layer was conducted to obtain the dataset of a boundary layer that approximates the profile of a neutral ABL at an offshore location. This data was then computed for use as an inlet condition for the ABL profile in the computational domain. Several methods in OpenFOAM were explored for this, such as use of the *groovyBC* function. The *groovyBC* function can be modified for differing mathematical expressions of the velocity and therefore can provide a good approximation to the generated ABL data in the wind tunnel experimentation. However the best approximation to the experimental data came from the *atmBoundaryLayerVelocityInlet* inlet condition (ABL inlet), which was modified to best approximate the experimental data. The ABL inlet generates a time-averaged horizontal velocity profile of the neutral ABL likely to be generated under the specified conditions. An example of the code for this inlet condition is shown in figure 8, which can be modified to account for differing values of freestream velocity (Uref), height of ABL being considered (Href), direction (n, z), relative surface roughness (z0) and height from which the ABL is being simulated (zGround).

```
inlet
{
    type            atmBoundaryLayerInletVelocity;
    Uref            10;
    Href            250;
    n               (1 0 0);
    z               (0 0 1);
    z0              0.01;
    value           $internalField;
    zGround         0;
}
```

Figure 8. – Example of Code for *atmBoundaryLayerInletVelocity*

The main consideration in generating the ABL was the defining of the relative roughness z0, the value of which can significantly affected the ABL profile generated. Figure 9 shows the effect of differing values of relative roughness. The value of z0 decided for use was 0.01, as this value corresponded the best to the experimental data.

Figure 9 - ABL Profile with differing roughness
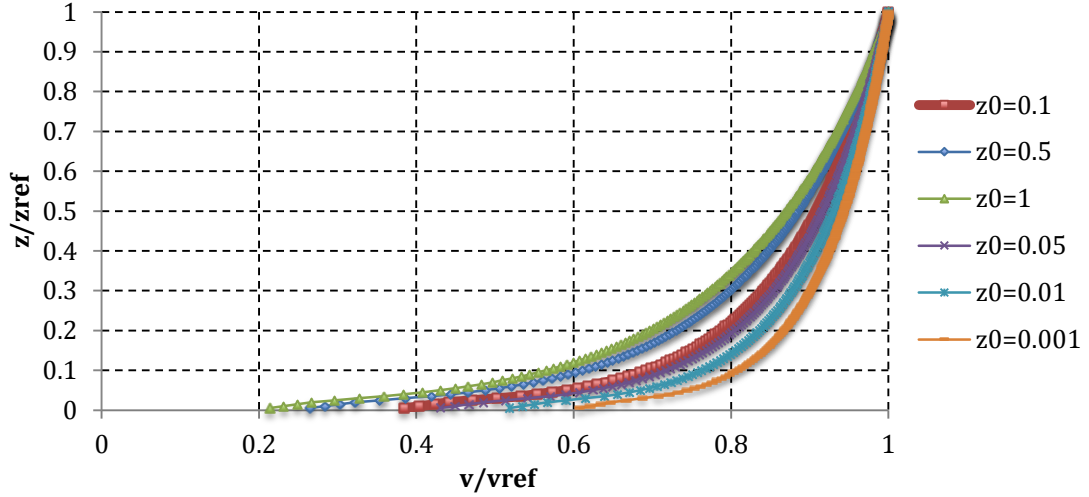
ABL Profile Comparison using NREL ABLSolver

As stated in the literature review, the ABLSolver developed by the NREL was used as a method for comparing the ABL profiles generated via the wind tunnel experimentation and the computational cost of the SEM used in this project. The ABLSolver is developed out of the buoyantBoussinesqPisoFoam solver in OpenFOAM 1.6; this approach was used to account for the thermal and buoyancy effects within the ABL. The theory of the ABLSolver will only be outlined in this report and is fully available at the NREL website [29], this is due the extensive theory of ABLSolver, which accounts for factors listed below.

- Time rate of change - $\frac{\partial \bar{u}_i}{\partial t}$

- Convection - $\frac{\partial}{\partial x_j}\left(\bar{u}_j \bar{u}_i\right)$

- Coriolis force due to planetary rotation - $2\varepsilon_{i3k}\Omega_3\bar{u}_k$

- Density-normalised pressure gradient - $\frac{\partial \tilde{p}}{\partial x_i}$

- Horizontal-mean driving pressure gradient - $\frac{1}{\rho_0}\frac{\partial}{\partial x_i}\bar{p}_0(x,y)$

- Stresses (viscous +SGS/Reynolds) - $\frac{\partial}{\partial x_j}\left(\tau_{ij}^D\right)$

- Buoyancy - $\frac{gz}{\rho_0}\frac{\partial}{\partial x_i}\rho_b$

- Other density-normalised forces (from actuator line model) - $\frac{1}{\rho_0}f_i^{T}$

The momentum transport equation for ABLSolver accounts for the previously mentioned factors and is defined as in equation 23:

$$\frac{\partial \bar{u}_i}{\partial t} + \frac{\partial}{\partial x_j}(\bar{u}_j\bar{u}_i) = -2\varepsilon_{i3k}\Omega_3\bar{u}_k - \frac{\partial \tilde{\rho}}{\partial x_i} - \frac{1}{\rho_0}\frac{\partial}{\partial x_i}\overline{p}_0(x,y) - \frac{\partial}{\partial x_j}(\tau_{ij}^{D}) - \frac{gz}{\rho_0}\frac{\partial}{\partial x_i}\rho_b + \frac{1}{\rho_0}f_i^{T}$$ - Equation 23.

Due to the factors incorporated into the model, the ABLSolver can simulate the ABL for neutral, stable and unstable conditions. For the scope of this project, only the neutral ABL was considered and modelled using LES. Figure 10 shows the 1km x 3km x 3km domain initialised by the implemented ABLSolver in this project. Figure 10 also shows the same domain geometry generated by the ABL inlet velocity using RANS modelling. This highlights the necessity of introducing turbulence into this domain for a better representation of the ABL.
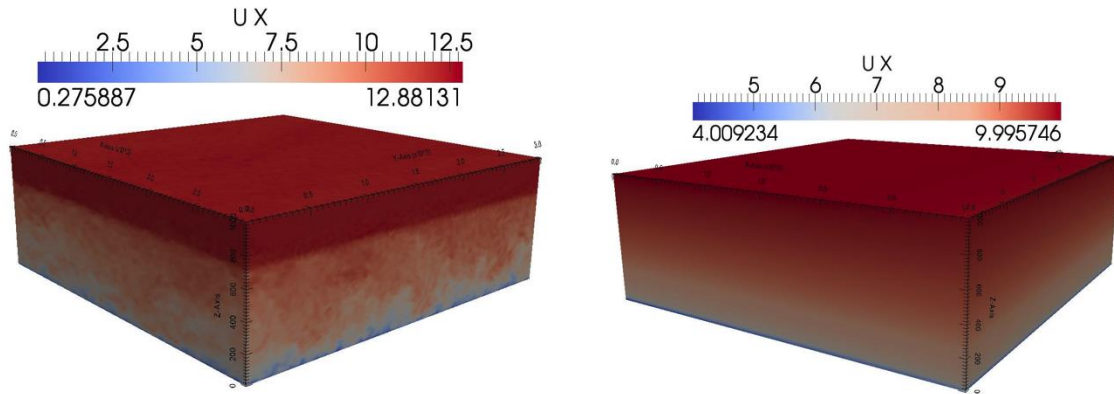
Figure 10. – Domains of generated ABLs from NREL solver and ABL inlet velocity

Turbulence Generation

With the Reynolds number of ABL flow being $\sim 10^{6}$, it is a very turbulent flow. As turbulence is a complex fluid motion composed of random coherent motions, the generation of turbulence into the domain must also be random, as any time-varying structured flow is not representative of the actual transient turbulence within the domain. The generated turbulence must also be preserved and not averaged because of the viscosity effects of a fluid simulation. Three main methods of introducing turbulence into the domain were considered at the beginning of the project, these being random noise, sinusoidal turbulence and the SEM.

The generation of random noise about a mean distribution at the domain inlet is the simplest method of introducing turbulence into the domain. Within OpenFOAM the inlet condition *turbulentInlet* produces random noise. This boundary type has filtering to preserve its spatial coherence. Filtering allows the creation of coherent structures such as eddies spatially and temporally, this allows a turbulent length scale to be specified. A velocity contour plot obtained from use of the *turbulentInlet* condition for the modelling of an ADM is shown in figure 11.
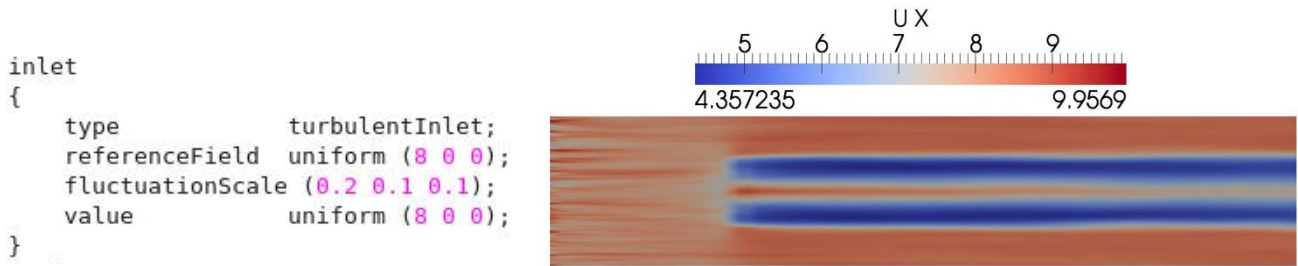
Figure 11. –*turbulentInlet* condition for actuator disk case

The SEM was considered favourable over sinusoidal turbulence because the turbulent eddies could be easily superimposed onto the mean velocity profile generated by the ABL inlet, which was decided as the most suitable method of generating the ABL profile. Also the turbulence produced by the SEM similar to that of using random noise, whilst also representing the range of frequencies and length scales that are likely to exist in physical turbulence. This is visible in figures 12 and 13, which show the distribution of eddies at the inlet of two cases simulated in this project using random noise and the SEM with mean ABL flow respectively.

Figure 12 and 13 – Comparison of eddies generated at inlet using random noise (left) and SEM (right)

From implementing the SEM, the turbulent ABL was then simulated for a height of 200m by using the SEM with the ABL inlet. This will be discussed in a later section.

20

Implementing New Solver/Modified SEM

In order to incorporate the behaviour of the ADM into the turbulent ABL profile described previously, it was decided to implement a solver that simultan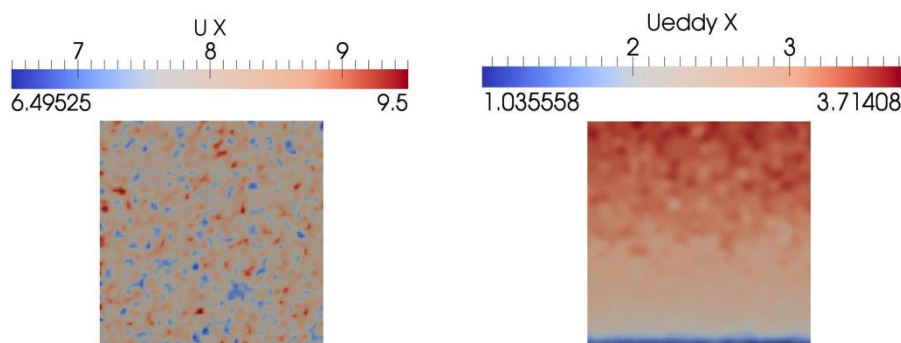eously resolves the behaviour of the actuator disk whilst also generating eddies at a specified location. The produced solver was called *EddiesAndActuatorDiskPisoFoam (EAADPF).*

Using *EAADPF* in conjunction with the steady-state ABL velocity profile inlet condition produced a resolved flow of the turbulent ABL with the ADM included. Figure 14 shows one of the simulations run for validating the use of this solver, with the value of *Ueddy* being half the sum of the mean flow velocity and the velocity of the eddies.
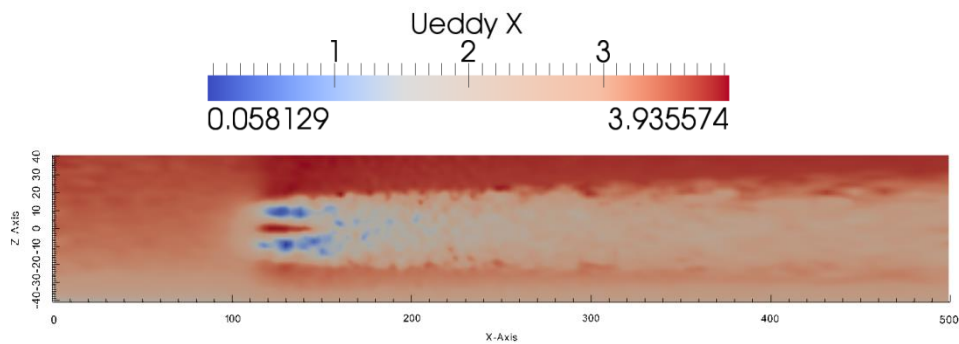
Figure 14. – Contour Plot of the Implemented EAADPF

The final solver produced has the ability of modifying the height of the ABL being analysed, the number of actuator disks, size of the actuator disks, the thrust and torque of the actuator disk and the characteristics of the eddies present within the domain.

In addition to incorporating an actuator disk, a control volume was utilised to calculate the power removed from the flow due to the presence of the ADM by using the *topoSet* and *setsToZones* utilities in OpenFOAM. The calculated power that was removed from the flow was then equated to the power produced by the turbine model, yielding an approximation to the power generation by a wind turbine of the same radius as the actuator disk at similar torques and thrusts. The momentum fluxes on each face of the control volume were calculated and then computed by a spreadsheet to calculate the power of the turbine. As the velocity subjected to the control volume varies with height with the ABL being simulated, the velocity is averaged over the cross-sectional area.

Final CFD Simulations

In order to relate the work of this project back to the group objective of evaluating existing modelling techniques, it was decided to compare the effect using of turbulent ABL airflow as opposed to a constant uniform inlet for modelling the behaviour of the ADM. An individual turbine as well as a turbine 10D (D=turbine diameter) downstream of the first turbine was considered for this investigation. The effect of the airflows was investigated by comparing:

- The average airflow velocity exposed to the ADMs
- The predicted power generated by the ADMs
- The wake structure of the ADMs

4. Presentation of Results

This section of the report covers the results relating to the wind tunnel experimentation of the project as well as the results of the CFD simulations in OpenFOAM.

4.1.   Wind Tunnel Experimentation

The data pertaining to the ABL profile from the wind tunnel experimentation can be summarised in table 2 and figure 15, which displays relative wind velocity as a function of relative height. This dataset was used as a basis for generating the offshore ABL profile in OpenFOAM and for proposing the most appropriate ABL inlet condition.

Table 2. – Induced Boundary Layer Experimental Data

h (m)	velocity (m/s)	z/zref	v/vref
0	0.00	0.00	0.000
0.001	0.95	0.01	0.172
0.002	2.43	0.02	0.440
0.005	3.62	0.05	0.656
0.010	4.06	0.10	0.736
0.020	4.43	0.20	0.803
0.030	4.87	0.30	0.882
0.040	5.18	0.40	0.938
0.050	5.23	0.50	0.947
0.060	5.31	0.60	0.962
0.070	5.36	0.70	0.971
0.080	5.43	0.80	0.984
0.090	5.52	0.90	1.000
0.100	5.52	1.00	1.000

Figure 15 - Velocity-Height Profile of Experimental data
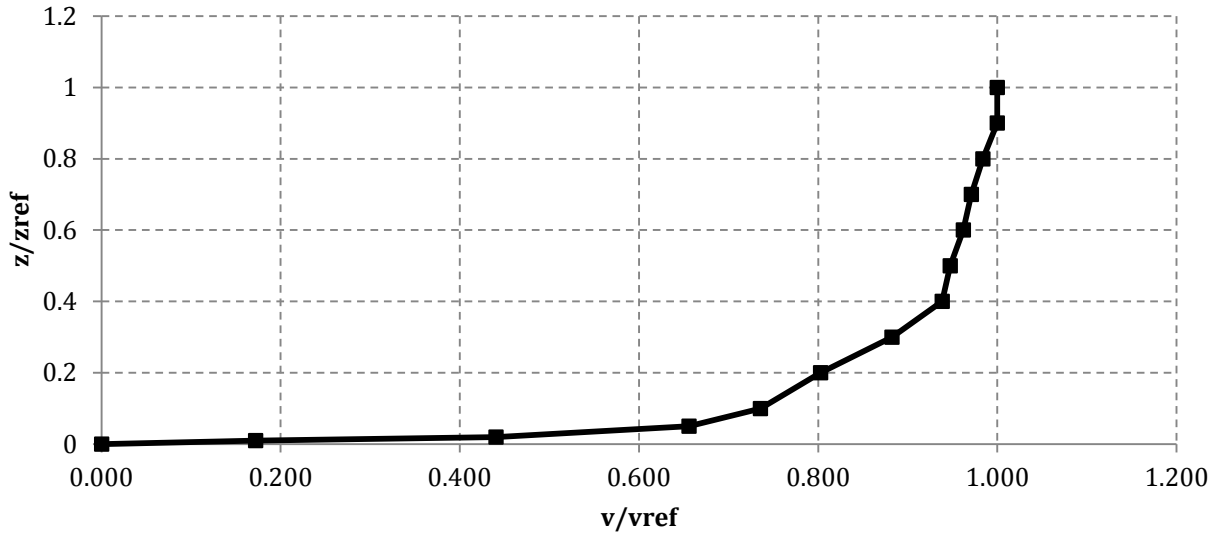
Using the velocities obtained at the heights of 2cm and 8cm (4.43m/s and 5.43m/s respectively), the Hellman exponent, α of the ABL profile was found by rearranging and computing the wind profile power law, equation 6. The value of the Hellman exponent, α, was found to be $\alpha = 0.147$. This shows the induced boundary layer is good approximation to the offshore ABL flow as the value of α typically varies between $0.1 - 0.16$ for offshore locations. From comparing the differing ABL profiles generated using the differing values of roughness, z_0 it was found that a value of $z_0 = 0.01$ was the most appropriate, this is higher value that what is usually considered for offshore. In addition to attaining an approximation to the profile of the ABL, the turbulent intensity of the airflow was calculated at differing heights. This was achieved using the equations described previously for processing a dataset of fluctuations that occurred over 30 seconds. These results are presented in section 4.2 and were used as a means of assessing the velocity field of the ABL profile in OpenFOAM.

4.2. ABL Profile Generation and Comparison

As mentioned previously, there were three approaches used for approximating the behaviour of the ABL. These were the wind tunnel experimentation of an induced boundary layer, the proposed SEM-ABL inlet method, and the ABLSolver. Figure 16 displays the differing ABL profiles generated, the CFD methods considered an ABL height of 1km.

23

Figure 16. – Comparison of the ABL Profile Generation Methods
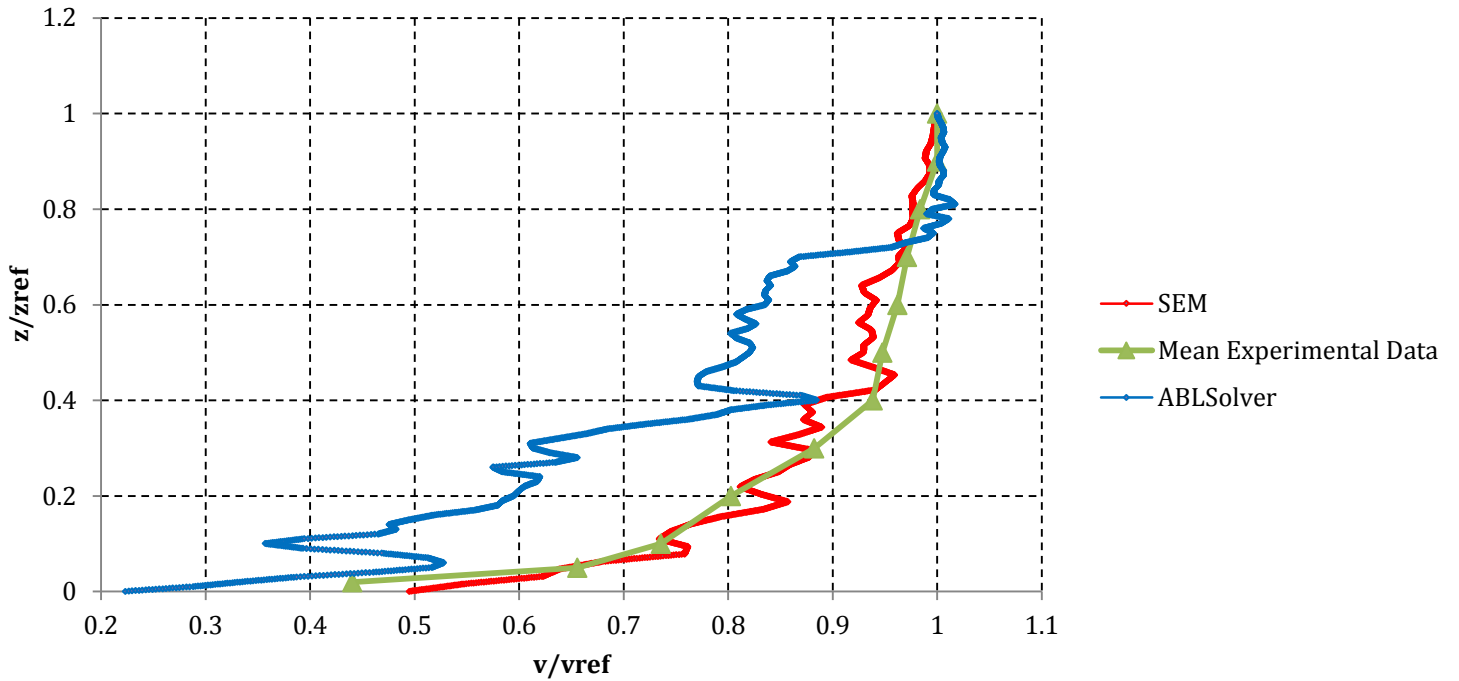
As is visible in figure 16, the ABL produced in OpenFOAM using the ABL inlet condition and the SEM correlates well with the boundary layer produced in the wind tunnel experimentation. However it is also shown that the ABLSolver produces a significantly lower approximation to the velocity of the airflow in sub-layer of the ABL. There are several possible reasons for this, with the effects of buoyancy and the Coriolis force being the most likely. Simulating the turbulence within the ABL to a height of 1km using the SEM was found to take several days to be fully developed. Due to this, and the wind turbine area of interest being a limited height, it was decided to only simulate the first 200m of a 1km high ABL. Figure 17 shows two velocity contour plots, the 200m high domain initialised with a turbulent ABL using *eddyPisoFoam,* and the resolved flow of a 1km high domain using *ABLSolver.*
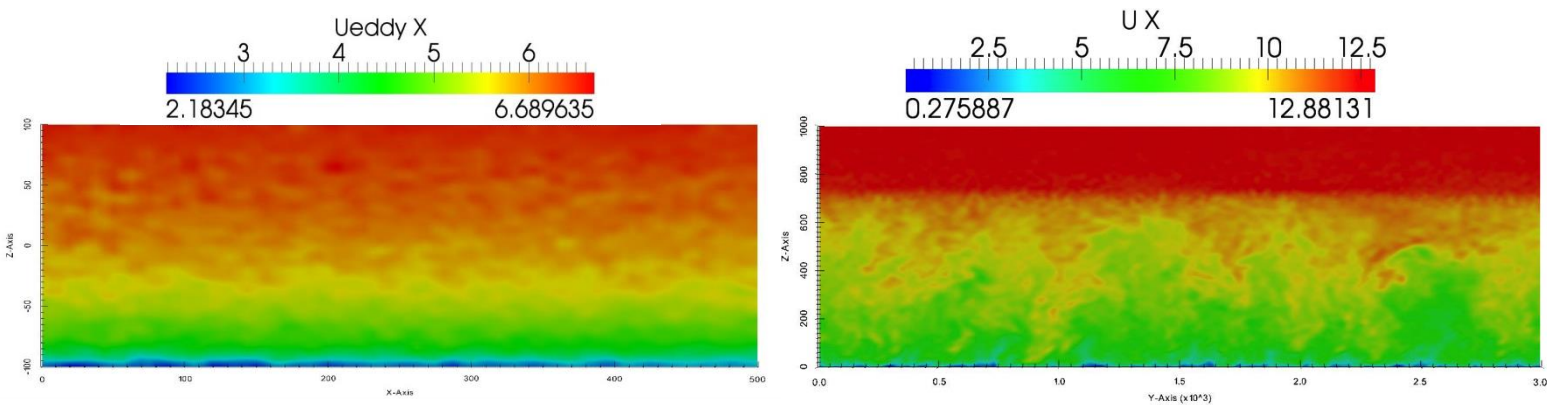
Figure 17. – ABL velocity profile using SEM-ABL inlet (left) and ABLSolver (right)

The method of using a SEM in conjunction with a mean ABL profile was further compared to the ABLSolver by evaluating the turbulence intensity of the flow at varying heights in the domain. The fluctuations about the mean velocities obtain in the wind tunnel experimentation were also considered, but were somewhat limited by the precision of the pitot-static tube. Figure 18 shows the turbulence fluctuations about the mean flow obtained at a height of 300m for the CFD methods and a reference height of 0.3 for the wind tunnel experimentation. Figure 19 displays how the turbulence intensity varies with the height of the generated ABL profiles.

Figure 18 - Turbulent Fluctuations over time for differing ABL Profiles
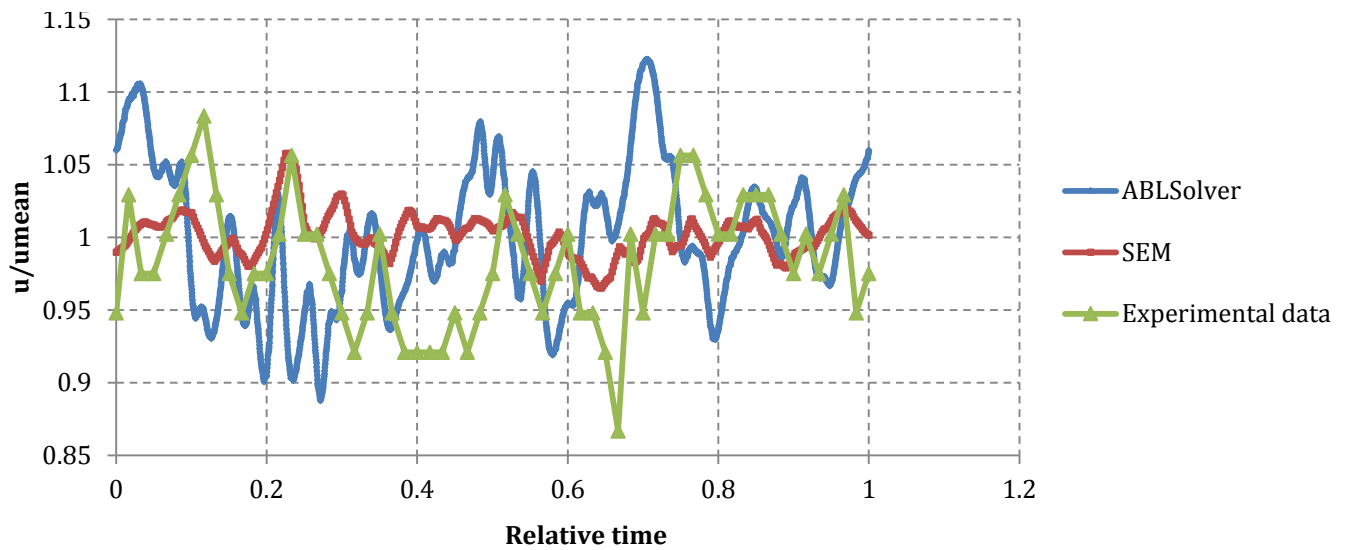
Figure 19 - Turbulence Intensity as a function of relative Height
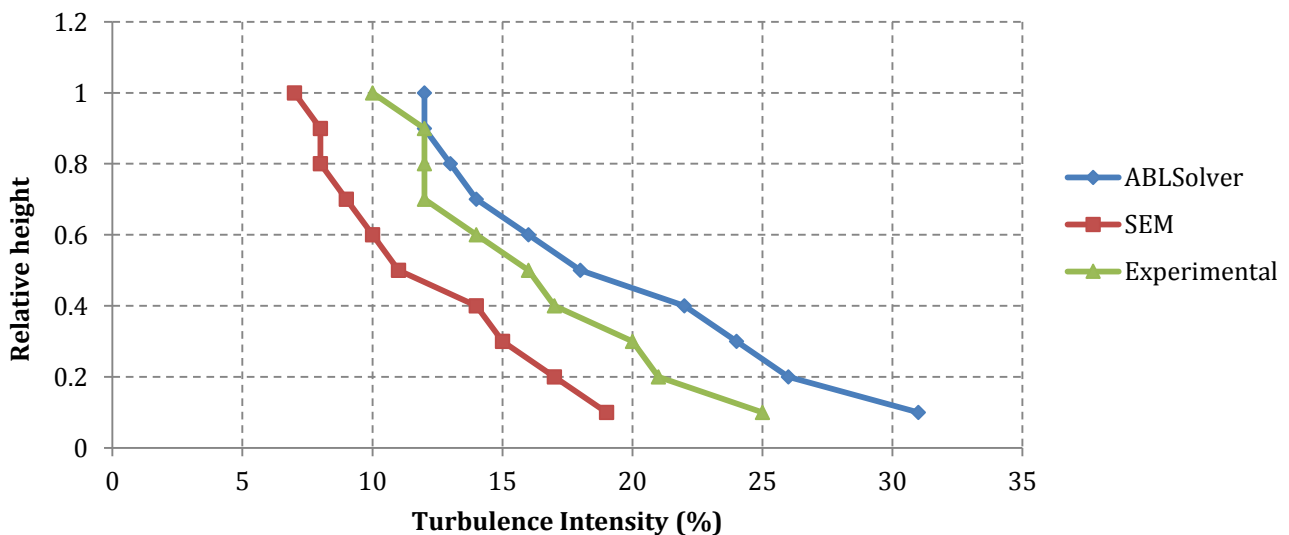
As is visible in figures 18 and 19, the SEM method produces a lower approximation to the fluctuations within the ABL compared to that of the ABLSolver and the experimentation. In order to validate and evaluate the accuracy of these two methods it is necessary for a real case to be studied and the results to be compared with actual offshore wind speed data. Despite this, it can be presumed that the ABLSolver produces a better approximation to actual ABL flow due to its high fidelity. However, as the scope of this project aimed to reproduce the wind tunnel data, the SEM was a valid method as it produced similar fluctuations.

In addition for being a suitable method for producing representative data of the boundary layer in the wind tunnel, the SEM-ABL inlet method was a more appropriate method for the time restrictions of the project. Table 3 shows the comparative simulation times of the NREL ABLSolver and the SEM.

Table 3 - Simulation Information of SEM-ABL inlet and ABLSolver

ABL Generation Technique	SEM/ABL Inlet	ABLSolver
Domain Size	800m x 100m x 200m	3km x 3km x 1km
Meshing Method	blockMesh	
Number of Cells	540,000	7,840,000
Notable Boundary Conditions	symmetryPlane	Cyclic
Run type	Standard	Parallel
Number of Cores/Processors	1/1	1/12
Simulation Time (hours)	~24	~254

4.3.   Effect of Turbulent ABL on Actuator Disk Model Behaviour

From generating a reasonable approximation to the ABL generated in the wind tunnel experimentation in OpenFOAM, the effect of using the turbulent ABL for simulating the behaviour of an ADM was investigated. LES modelling of the turbulent ABL and ADM was compared with the RANS modelling of the same ABL profile, and a uniform inlet for the same ADM. The k-epsilon model was used for the RANS modelling. The two approaches were compared by assessing; i) the average airflow velocity exposed to the ADM at the turbine height ii) the predicted power generated by the turbine model and iii) the wake structure of the ADM. Table 4 lists the characteristics of the ABL and uniform inlet conditions being assessed. For this investigation an individual turbine was considered as well as an identical ADM 10D downstream of the first turbine.

Table 4. – Table of Assumptions and Constants

Quantity	Uniform Inlet	ABL RANS	Turbulent ABL
	Value		
Flow	Incompressible		
Inlet Velocity	8m/s	ABL Inlet, Uref=8m/s, Href=1000m	
RANS/LES	RANS		LES
Turbulence Model	k-epsilon		Smagorinsky sub-grid
Interior radius of ADM	1.5m		
Exterior radius of ADM	20.5m		
Thrust of ADM	4.75E+04		
Torque of ADM	1.12E+05		
Density of ADM	1.25		
Start and end of 1st ADM	(110 0 0) to (120 0 0)		
Start and end of 2nd ADM	(310 0 0) to (320 0 0)		

4.3.1. Velocity of Airflow Exposed to Turbine

By use of a control volume, the average velocity of airflow exposed to the ADM at the turbine height of 100m was assessed. These results are summarised in table 5.

Table 5 - Velocity Exposed to turbine at 100m turbine height

Inlet Velocity	Velocity Exposed to turbine (m/s)	
	Individual turbine	10D downstream turbine
Uniform Inlet	8	5.83
ABL RANS	7.02	5.23
Turbulent ABL	7.04	5.22

As expected, the average velocity of the airflow is less when considering the ABL profile to that of the uniform inlet. This has little significance, but was mainly studied to show that the turbulence introduced into domain maintained the velocity characteristics of the flow.

4.3.2. Wake Structure Produced by Actuator Disk model

The wake behind a wind turbine can be divided into the near and far wake regions. The near wake region is strongly influenced by the rotor shape and the blades of the wind turbine; this includes the tip vortices shed from the blades. The far wake region of the turbine is less important but can be significant when considering the airflow exposed to downstream turbines. This section presents a visual and quantitative analysis for the flow of the fluid-turbine interaction using an ADM. Figure 20-23 shows velocity contour plots of the final simulations conducted in this project, with the blacked out regions representing the presence of an ADM.
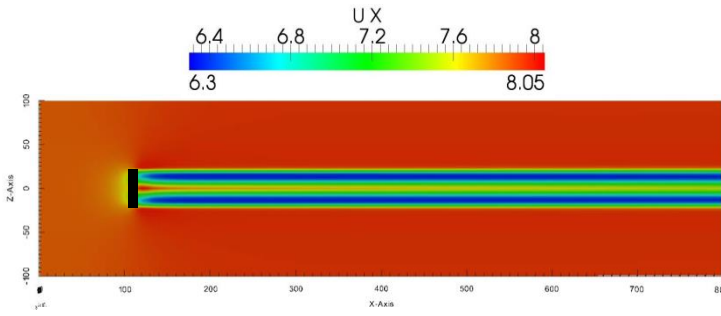
Figure 20 – RANS Modelling of individual ADM
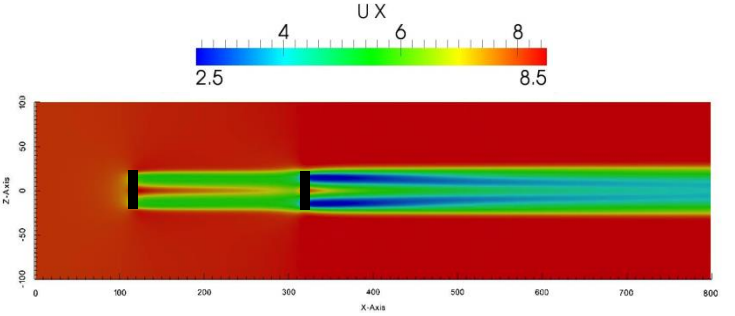
Figure 21 – RANS Modelling of two ADMs
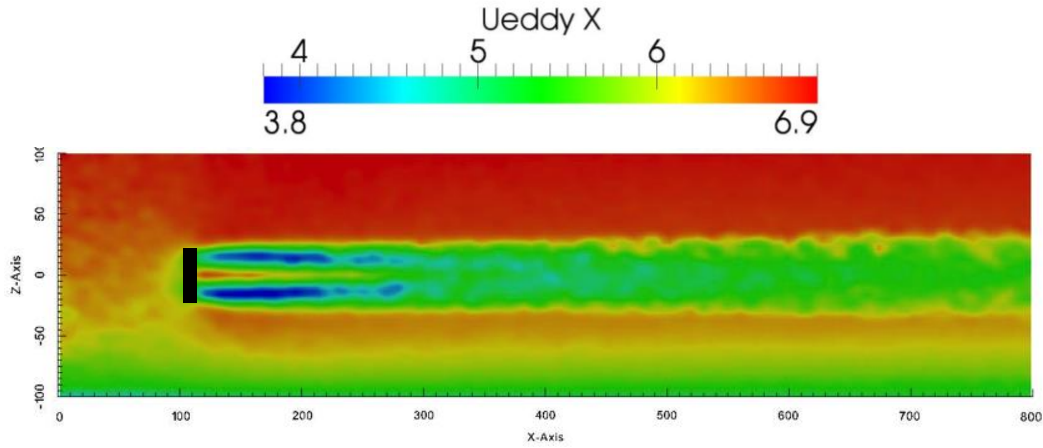
Figure 22 – LES Modelling of individual ADM with turbulent ABL
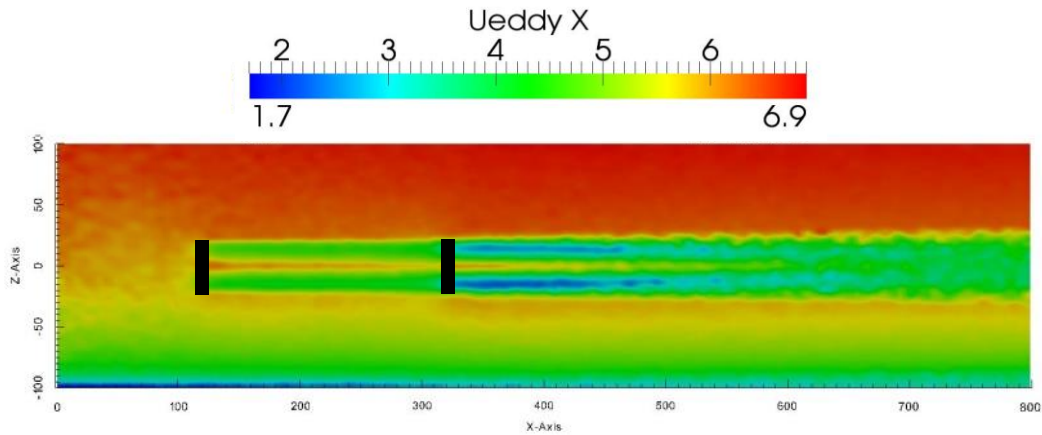
Figure 23 – LES Modelling of two ADMs with turbulent ABL

As expected, the downstream turbines are exposed to a lower airflow velocity due to them being in the wakes of the first turbine. The effect this has on the power generated from the ADM is presented in the following section. As visible in the contour plots, the main benefit of using LES modelling and using the turbulent ABL airflow is a better representation of the wake expansion of the turbines. This is more evident in lower velocity airflows such as the previously seen implementation in figure 16. Wake expansion is thought to be a significant part of the current turbine performance issues in the wind energy industry and therefore the use of this

28

model for assessing more downstream turbines could be very useful. Also visible in the contour plots is the main drawback of the ADM, which is that the flow of the near wake region is notably simplified, with no effect of tip vortices being present. The wakes generated by the ADM for these simulations have been plotted in figures 24-27, this was achieved by sampling the velocity downstream of the turbine were across the z-direction of the domain at four different distances. *D* represents the turbine diameter.

Figure 24 - 1D Downstream
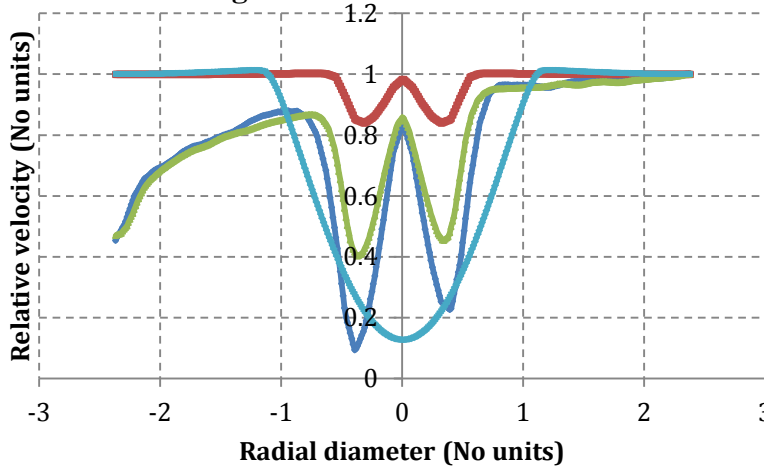
Figure 25 - 2D Downstream
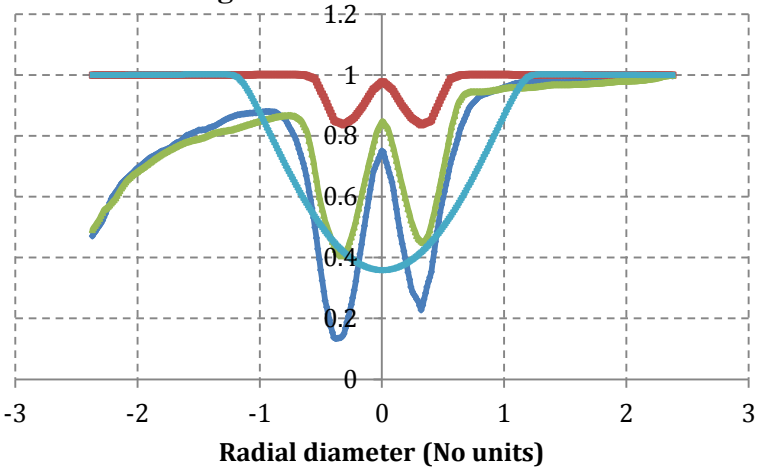
Figure 26 - 4D Downstream
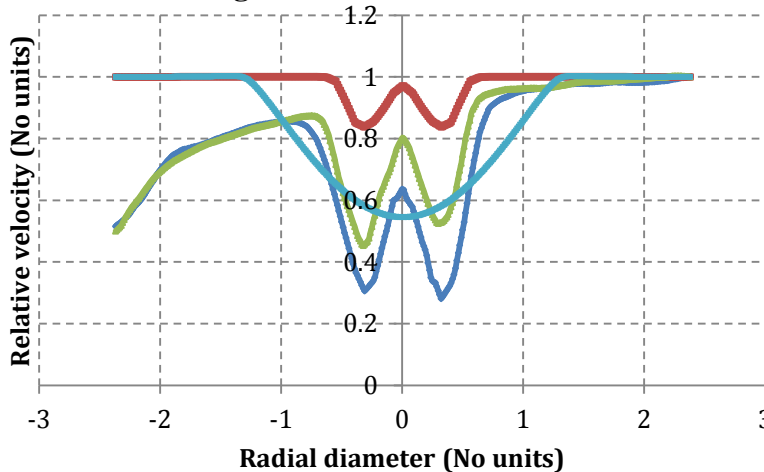
Figure 27 - 6D Downstream
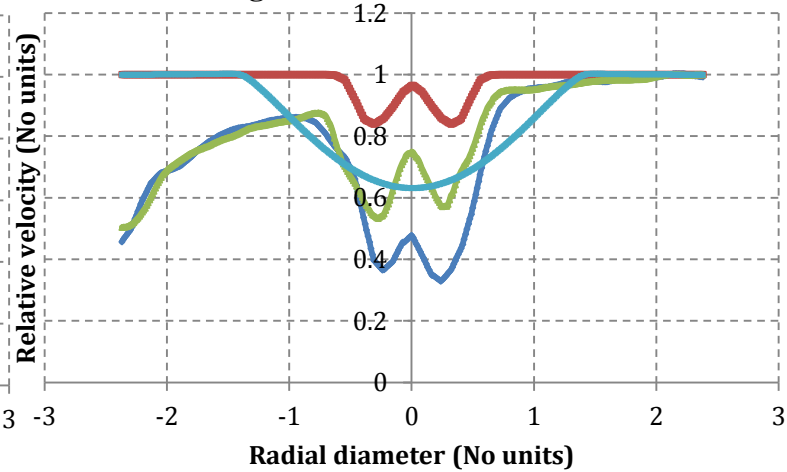
— 2nd Turbine Turbulent ABL — 1st Turbine Uniform
— 1st Turbine Turbulent ABL — 2nd Turbine Uniform

Figures 24-27 shows that the use of the ABL generates a non-axisymmetric distribution of the velocity field downstream of the turbine interaction. Additionally, the wakes behind the second ADM using the different inlets are not very similar in magnitude. Using RANS modelling, the wake is wider and the minimum velocity is greater, especially when considering the far-wake region. It is also clearly noticeable that the near-wake of the ADM when using the turbulent

29

ABL is very similar when considering the 1st and 2nd turbine. However the velocity wakes is less similar when considering the far-wake region. This similarity in the velocity of the near wakes is likely due to the ADM, which struggles with providing indicative results in the near wake region. This highlights the necessity of utilising an ALM as opposed to an ADM for improved modelling of the near wake region of wind turbines.

4.3.3. Power Generated by Actuator Disk Model

Using a control volume that encompassed the region of the actuator disk and assessing the momentum of the fluid lost through the fluid-turbine interaction obtained the predicted power generated by the ADM at the specified torque and thrust for the differing airflows. The results are shown in table 6.

Table 6. – Power Generated for the turbines for the differing simulations

Inlet Velocity	Power Generated (W)	
	Individual turbine	10D downstream turbine
Uniform Inlet	1591621	1173287
ABL RANS	1459274	1074382
Turbulent ABL	1456967	1072273

As with the assessing of the velocities exposed to the wind turbines, the uniform inlet predictably produced a greater power generated. The aim from assessing the difference in the power generated when using a uniform inlet with that of the turbulent ABL was to establish the maximum difference in power that could be being approximated by simplifying or ignoring the effects of the ABL. This difference in power between the turbulent ABL and uniform inlet simulation in this paper was found to be 9.24%, further study of a wider range of models and wind speeds will be necessary to validate this.

5. Discussion and conclusions

5.1. Discussion and Conclusions

At the onset of the project, the aims for this individual project were to:

- Approximate the velocity profile of an offshore ABL via wind tunnel experimentation
- Incorporate an ADM into the domain of the turbulent ABL by modifying a SEM.

- Assess the impact of using turbulent ABL flow as opposed to a constant uniform inlet velocity for the ADM

In the Wind tunnel experimentation component of the project a boundary layer was induced to replicate the profile of an ABL likely to be encountered at offshore wind farms. The produced boundary layer adhered well with the expected profile of the expected ABL, having a Hellman exponent of 0.145 which is similar to offshore locations [26]. This data was replicated as an inlet in OpenFOAM by the ABL inlet velocity condition and used as the mean flow on which synthetic turbulence was introduced via the SEM. Imposing synthetic turbulence onto this ABL inlet produced a turbulent velocity-height profile with similar fluctuations to that of the ABLSolver whilst adhering to the data of the wind tunnel experimentation, successfully transferring wind tunnel data to OpenFOAM. Analysing the turbulence intensity within the flow also validated this. However, actual offshore wind data is necessary to confirm the validity of this approach.

The SEM was then modified to also model the effect of the ADM, fulfilling the second objective of the project by creating EAADPF. The main issues when incorporating the SEM with the ADM were compiling errors, the most significant of which was the dimensions of phi not being compatible between the models. This issue was resolved and the effect of the turbulent ABL on the ADM was then assessed and compared to the use of a steady-state inlet.

From the CFD investigation of the project, the conclusions that can be drawn regarding the effect of the turbulent ABL on the ADM performance are somewhat limited. The velocity exposed to the turbine was found to be very similar for the RANS and LES simulations of the ABL as expected, with the uniform inlet predictably being higher. These differing airflow velocities translated into a corresponding power generation, with the uniform inlet producing 9.24% more power than the turbulent ABL. And much like the velocities, the power generated using the RANS and turbulent ABLs were very similar. The same was found to be true for the downstream turbines. The conclusion from this part of the investigation was therefore that for the modelling of 1-2 turbines, it is only necessary to calculate the velocity of the airflow at the turbine height for assessing the power generated by the turbines. This can be done using the ABL inlet or by calculating the airflow at the turbine height and using this velocity as a uniform inlet.

The main results of interest from the investigation came from the wakes generated by the turbines. It was found that the ABL flow influences the velocity of the airflow exposed to downstream turbines much more significantly than the uniform inlet due to the non-axisymmetric velocity distribution produced in the wake of the turbines. This could be significant for the power generated by wind turbines further downstream. Additionally, the issue of the ADM limitations in the near wake region were significant, indicating that turbulent ABL flow is only necessary for more sophisticated models such as the ALM. However, the study of the ADM wakes in the near and far wake regions still suggest that the modelling of the turbulent ABL is still a vital part of wind farm modelling.

5.2.   Further Work

In order to better clarify the accuracy of the method used in this project more validation is required. This can be achieved by refining the mesh, especially at the inlet for examining the turbulent length scale of eddies which are limited by mesh density. Smaller time steps will also be necessary for this. Additionally, to overcome the issue of the somewhat limited analysis of the near wake modelling, an ALM should be used as opposed to an ADM. This has been proven in other areas of the group work.

Apart from this, the proposed methods still has its limitations and therefore minimising these limitations should be the primary focus of further work. Even though the ABL inlet condition can simulate a neutral offshore ABL, this approach does not account for factors of the flow such as buoyancy which can be significant when considering a full array of turbines. This was highlighted by comparing the profile generated by the ABL inlet with that of the ABLSolver, which is likely to produce a better approximation to the ABL. To minimise this, the SEM-ABL method could be further modified to incorporate an extra term to account for some of the currently omitted factors.

Another way of developing EAADPF, would be to greater define the characteristics and behaviour of the generated eddies. Among these characteristics would be the specification of the eddy length scale with respect to position and time within the flow and how they interact with boundary conditions, this may aid the computational expense of the method. Varying the angle of the airflow exposed to a turbine was also considered in the project, unfortunately the time restrictions of the project meant that the constructed mesh, figure 28, was not used for simulating the ABL. The mesh was constructed so that changing wind angles would have no

bias from the mesh.
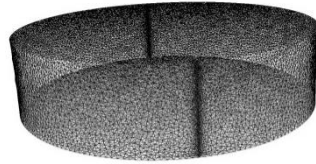
Figure 28. – Proposed Cylindrical Mesh

In conclusion, using EAADPF in conjunction with a mean ABL inlet can be considered as a good approximation to the atmospheric airflow exposed to wind farms and should be considered as an option for commercial CFD wind turbine simulations. Use of EAADPF has produced good approximations of the wakes that are likely to occur. However, further work, offshore wind speed data and experimentation is required to investigate if this method produces better approximations to the observed behaviour of wind turbines that current modelling techniques. The capabilities of the model to predict the power generated from wind turbines is also a key area of interest and further validation. As such, with further evaluation and modification of the model, the model has the possibility of producing improved approximations to the fluid-turbine interactions. Despite this, ABL solvers that account for buoyancy, temperature and Coriolis force, such as the ABLSolver are still preferable if the computational resources and timeframe is available.

6. Project management

6.1.   Time Management and Gantt Chart

The progress of the project was monitored via a Gantt chart that was constructed at the commencement. The work within the project was sub-divided into work packages, displayed in the Gantt chart. The Gantt chart was utilised so that the milestones and deliverables key to the completion of the project were met in a timeframe that ensured the work was completed in time. Tracking and allocating the tasks within this project is particularly necessary as a large percentage of the project deals with CFD, CFD simulations can take several hours, days or weeks and therefore a conservative timeframe is given to the duration and setup of the CFD cases being simulated. Doing this allowed time for alternative approaches to be considered for problems encountered throughout the project. The Gantt chart was modified throughout the project to account for changing elements within the project, the final Gantt chart of the project is shown in figure 29.

Figure 29. – Gantt Chart for Management of Project

Project Planner

Period Highlight 29 | Plan | Actual | % Complete | Actual (beyond plan) | % Complete (beyond plan)

ACTIVITY	PLAN START	PLAN DURATION	ACTUAL START	ACTUAL DURATION	PERCENT COMPLETE
Reports and Presentations					
G1 Group Report	1	2	1	2	100%
I1 Report	4	6	4	6	100%
G2 Group Report	24	5	24	5	100%
I2 Report	19	10	19	10	100%
Peer Assessments	28	1	28	1	100%
Poster Day	30	4	0	0	0%
Individual Project Deadlines					
Assignment of Project	1	2	1	2	100%
Literature review	2	8	2	8	100%
Implementation of Actuator Disk Model (ADM)	3	4	3	4	100%
Compiling NREL ABLSolver	6	3	7	4	100%
Setup of NREL ABLSolver	10	1	10	1	100%
Design and Construction of Wind tunnel Model	14	3	14	3	100%
Studying ABL Inlet Generation Methods	14	3	14	3	100%
Wind tunnel Experimentation	17	1	17	1	100%
Compiling and Implementation of SEM	18	2	18	3	100%
SEM and ABL Inlet Generation for Turbulent ABL	21	2	21	3	100%
Creating of New Solver (SEM and ADM incorporated)	21	4	21	4	100%
Apply Control Volume to Final Simulation Cases	24	1	24	1	100%
One Turbine Simulation Case	25	3	25	3	100%
Two Turbine Simulation Case	25	3	25	3	100%
Comparison of Power and Wake Structures of Cases	27	2	27	2	100%

The progression of the individual projects associated with the overall wind farm modelling group project was tracked at weekly meetings. These meetings comprised of all the group members, Steven Daniels and Gavin Tabor, the project supervisor. The chair and secretary roles were rotated weekly with the meeting minutes and agendas being posted on the online sharing platform Google Drive.

6.2.   Risk Assessment and Health and Safety Concerns

Table 7 on page 36 shows the risk assessment table for this project. This table outlines the main issues encountered and negotiated during the course of the project. The main concerns regarding the aims of the project not being met were due to the complexity of the CFD models being considered. The complexity of the CFD models influences the setup and therefore run-time of the CFD simulations. Some of these factors include the mesh density of the domain, the solver, the selected timestep and the complexity of the flow being considered. These are outlined in the risk assessment table.

The health and safety concerns of this project mainly arose in the wind tunnel experimentation conducted in this project and are outlined in tables 8 and 9, also on page 36. The health safety concerns in the rest of the project were minimal as the work was almost all computational, it is

advisable however to take regular breaks from working with the computers to avoid eye strain and repetitive strain disorder.

6.3.   Sustainability, Repercussions of Work and Budget

As stated previously, wind energy is currently the most viable alternative energy source to fossil fuels, but the power generated from wind turbines is currently less than that predicted by wind turbine models. Superior modelling of the various aspects of wind farm aerodynamics therefore has the capability of providing a better understanding of the aerodynamic interactions within wind farms. This will lay the foundations of minimising the power discrepancy by proposing better geographical locations of wind farms, better configurations of wind farms and potentially better wind turbine designs. These outcomes will make wind energy more viable. As wind energy is a much more sustainable source of energy compared to fossil fuels the current rate of pollution will also be reduced, providing that the cost per unit energy of using wind turbines is less or similar to fossil fuels.

In terms of the sustainability within the project, CFD is a much more sustainable approach to modelling wind turbine aerodynamics than using wind tunnel experimentation. This is because CFD simulates the wind flow without having to construct multiple models for wind tunnel testing, this saves material and the costs of using the wind tunnel.

The budget allocated to the group project was £800. The expenditures incurred throughout the group project only came from manufacturing the roughness elements and spires for generating the profile of the ABL for the wind tunnel experimentation. The cost of constructing the wind tunnel model was minimal and did not make a significant impact into the group budget due to the majority of the materials being recycled.

Table 7 – Risk Assessment table

Risk Item	Cause	Effect	Likelihood (low 1 – high 5)	Severity (low 1 – high 5)	Importance (Likelihood x severity)	Action to minimise risk
Implementation of Actuator Disk Model	Unfamiliar with using OpenFOAM	Consequent and dependent work tasks delayed, jeopardise the work of the project	1	5	5	Study and understand the workings of OpenFOAM. Particularly the use of non-standard solvers.
Wind tunnel experimentation not providing useful results	Constructed roughness elements and spires not effective	ABL profile dataset not obtainable in sufficient time. Delays project	3	3	9	Begin wind tunnel experimentation early in project and adjust spires and roughness elements
Compiling and Implementing SEM	Problems with the SEM solver code.	Turbulence not generated in the domain, requires alternative approaches to be considered	3	4	12	Give sufficient time for compiling the SEM and seek assistance from supervisors where appropriate
Compiling EAADPF	Incompatibilities between the code of the SEM and the actuator disk model	Unable to produce solver for simultaneously modelling turbulence and the ADM. Alternative approach required.	3	4	12	Conservative time allocated to task which encountered several complications, namely the dimensions of several quantities
Simulation run time	Computational cost of solvers is excessive for the timeframe of project	Simulations do not yield sufficient results	2	5	10	Conservative time given to simulations

Tables 8 and 9 – Health and Safety tables

Hazard	Existing control measures	Score A	Score B	Risk (AxB)
General workshop environment	Technician present in workshop hours. Wearing safety equipment provided.	2	2	4
Damage to ears by excessive presence using wind tunnel	Take regular breaks. Use ear protection.	1	2	2
Damage to eyes from foreign particle in wind tunnel	Wear safety goggles correctly.	1	1	1
Sharp and Power tools in workshop	Handle with care.	2	3	6

Injury probability (A)	Score A	Injury severity (B)	Score B
Small chance	1	Slight injury	1
Unlikely	2	Minor injury	2
Possible	3	Major injury	3
Probable	4	Severe injury	4
Very likely	5	Death	5

7. Contribution to group functioning

7.1.   Group Structure

In the 'Wind Farm Modelling' Group project there were nine students who were divided into two sub-groups for investigating possible causes for the power discrepancy between the observed and modelled power generated from wind farms. The focus of these two sub-groups were to:

- Evaluate existing modelling techniques for wind farm modelling
- Research future improvements for wind farm modelling techniques

The work conducted in this project was considered as part of the group for evaluating the existing modelling techniques for wind farm modelling. In this sub-group, the same Goldstein optimum distribution for the ADM was used in all the CFD components of the group's work. This ensured that the factors investigated were solely responsible for the results attained from differing modelling techniques.

7.2.   Contribution to Group Work

This project work contributed to the overall group aim by indicating that the effect of modelling the turbulent ABL can be significant on the ADM aerodynamics and can be a significant contributor to the existing power discrepancy of wind farms when simplified. This has been proven by examining the wakes generated downstream of the ADM. Computing the power generated by the ADM also showed this. The power differential between using the turbulent ABL and a uniform inlet with the factors setup in this project was 9.24%. Additionally this project proposes a method used for generating the ABL whilst simultaneously modelling wind turbines via the produced *EAADPF* solver. This can be used for the other wind turbine models proposed in this project as well as future techniques.

This work therefore proposes a potential contribution to the reasons current models overestimate the power generated by wind turbines and a method of generating the turbulent ABL for future simulations of a limited domain height for differing turbine array geometries and wind turbine models.

1

References

[1] – Svenning, E. 'Implementation of an actuator disk in OpenFOAM' Chalmers University of Technology, 2010.

[2] –Jarrin, N. Benhamadouche, S. Lawrence D. and Prosser, R. 'A Synthetic-Eddy Method for Generating Inflow Conditions for LES' International Journal of Heat and Fluid Flow, vol. 27, pp. 585-593, 2006.

[3] – Lignarolo, L. Gorlé, C. Parente, A. Benocci, C. 'Large eddy simulation of the atmospheric boundary layer using OpenFOAM' 13th International Conference on Wind Engineering – Amsterdam, The Netherlands, 2011.

[4] – Sumner, J. Masson, C. Odemark, Y. and Cehlin, M. 'OpenFOAM simulations of atmospheric flow over complex terrain', 5th OpenFOAM Workshop, Chalmers, Sweden, June 21-24, 2010.

[5] – Garratt, J. 'The Atmospheric Boundary Layer', Cambridge: Cambridge University Press, 1992.

[6] – Holdaway, D. Tabor, G. Beare, B. 'An Examination of the Feasibility of Using OpenFOAM to Model Air Flow for Wind Turbine Positioning', College of Engineering, Mathematics and Physical Science, University of Exeter, 2011.

[7] – Blessmann, J. 'Simulation of the Natural Wind Structure in an Aerodynamic Wind Tunnel', Ph.D. thesis, Instituto Tecnológico de Aeronáutica (ITA), S.P., Brazil, 169 p, 1973.

[8] – Churchfield, M.J. Vijayakumar, G. Brasseur, J.G and Moriarty, P.J. 'Wind energy-related atmospheric boundary layer large-eddy simulation using OpenFOAM', Paper 1B.6 at the American Meteorological Society, 19th Symposium on Boundary Layers and Turbulence, National Renewable Energy Laboratory, Colorado, 2010

[9] – Andren, A. 'The structure of the stably stratified atmospheric boundary layer: A large-eddy simulation study', Quarterly Journal of the Royal Meteorological Society, 121(525):961–985, 1995.

[10] –Stoll, R. Porté-Agel, F. 'Effect of roughness on surface boundary conditions for large-eddy simulation', Boundary Layer Meteorology, 118(1), 169-187, 2006.

2

[11] – Chang, Y. Scotti, A. 'Modelling unsteady turbulent flows over ripples: Reynolds averaged Navier-Stokes equations (RANS) versus large-eddy simulation (LES)', Journal of Geophysical Research: Oceans (1978-2012), vol. 109, p. C09012, 2004.

[12] –Ferziger, J.H. and Peric, M. 'Computational methods for fluid dynamics, volume 2', Springer Berlin, 1999.

[13] –Jarrin, N. 'Synthetic Inflow Boundary Conditions for the Numerical Simulation of Turbulence', University of Manchester, Faculty of Engineering and Sciences, 2008.

[14] – Richmond, J. 'Inlet Conditions for Large Eddy Simulation of the Atmospheric Boundary Layer', College of Engineering, Mathematics and Physical Science, University of Exeter, 2015.

[15] – Churchfield, M. Lee, S. Moriarty, P. 'Overview of the Simulator for Wind Farm Application', National Renewable Energy Laboratory, 2012.

[16] – Irwin, H. 'The design of spires for wind simulation', Journal of Wind Engineering and Industrial Aerodynamics, 7, 361-366, 1981.

[17] – Campbell, G.S. Standen, N.M. 'Simulation of earth's surface winds by artificially thickened wind tunnel boundary layers', Progress Report II, National Research Council of Canada, 1969.

[18] – Counihan, J. 'A method of simulating a neutral atmospheric boundary layer in a wind tunnel', Proc. Advisory Group for Aerospace Research and Development, Conf. on the Aerodynamics of Atmospheric Shear Flows, 1979.

[19] – Hobson-Dupont, M. 'The Development of a Small-scale Wind tunnel Simulating the Atmospheric Boundary Layer.', San Jose State University, 2015.

[20] – Mikkelsen, R. 'Actuator disc methods applied to wind turbines', Department of Mechanical Engineering, DTU, Lyngby, 2003.

[21] – Sanderse, B. 'Aerodynamics of wind turbine wakes: literature review', Energy Research Centre of the Netherlands (ECN), 2009.

[22] – Horlock, J. H., 'Actuator Disk Theory', *McGraw-Hill Inc.*, 1978.

[23] – Gebreslassie, M. 'Simplified CFD Modelling of Tidal Turbines for Exploring Arrays of Devices', College of Engineering, Mathematics and Physical Science University of Exeter, 2012.

[24] – Sagaut, P. 'Large-eddy simulation for incompressible flows', Springer-Verlag, Scientific Computation series, 2005.

[25] – Leonard, A. 'Energy cascade in large-eddy simulations of turbulent fluid flows', Adv. in Geophysics, 1974.

[26] – Kaltschmitt, M. Streicher, W. Wiese, A. 'Renewable energy: technology, economics, and environment', Springer, 2007.

[27] – [Online] 'Note on the Body Force Propeller implementation in FINE^{TM}/Marine', Available at: http://www.tfd.chalmers.se/˜hani/kurser/OS_CFD/Actuator_Disk.pdf (Last accessed: 23/03/2016)

[28] – [Online] Hellman exponent values, Available at:

http://www.slideshare.net/Jupiter276/vl-wind-energymeteorologyss1102 (Last accessed:22/02/2016)

[29] – [Online] NREL Wind farm modelling solvers. Available at:

http://wind.nrel.gov/designcodes/simulators/sowfa/ (Last accessed:18/03/2016)